Pattern Formation Induced by Internal Microscopic Fluctuations

Hongli Wang,[†,‡,§] Zhengping Fu,[†] Xinhang Xu,[†] and Qi Ouyang*[,†,‡,§]

Department of Physics, and The Beijing-Hong Kong-Singapore Joint Center for Nonlinear and Complex Systems (PKU), and Center for Theoretical Biology, Peking University, Beijing 100871, China

Received: November 9, 2006; In Final Form: December 15, 2006

We report spatiotemporal patterns induced by microscopic fluctuations in the Gray−Scott model. In the framework of stochastic kinetics, the macroscopic effect of internal noise of the system was investigated by simulating the reaction−diffusion master equation using Gillespie's algorithm. Pattern formation at the level of stochastic description is presented in comparison with that given by deterministic equations. Complex spatiotemporal patterns, including spiral waves, Turing patterns, self-replicating spots and others, which are not captured or correctly predicted by the deterministic reaction−diffusion equations, are induced by internal reaction fluctuations. Furthermore the intrinsic noise selects and controls the pattern formation with different intensities of fluctuation.

1. Introduction

It is well established nowadays that fluctuations can play constructive roles and lead to a rich variety of dynamical effects. Far from being a source of nuisance, noise can induce organized and counterintuitive dynamical behaviors. Well-known examples in zero-dimensional systems are noise-induced transitions[1] and stochastic resonance.[2] More recent examples in spatially distributed systems[3] include noise-induced phase transitions[4] and pattern formation,[5] noise-induced fronts,[6] wave nucleation,[7] and interaction of turbulence with noise,[8] to name only a few. Most works in this field have focused on external noises where the stochastic source is due to a fluctuating environment, which is coupled with the dynamical system. Another type of pervasive noise is the internal microscopic fluctuation due to the randomness in microscopic degrees of freedom. The internal noises, for instance, thermal fluctuations, are intrinsic and unavoidable in real systems. While the effect of external noises have been discussed extensively in spatially distributed systems, investigations of the influence of intrinsic microscopic fluctuations are mainly limited to low-dimensional systems.[9] Comparatively much less attention has been payed to the macroscopic effect of these fluctuations in pattern formation systems. Only a few reports available have considered mesoscopic pattern formation.[10−13] The purpose of this paper is to explore the influence of internal noise in reacting and diffusing systems. We show that internal fluctuations can drastically change the pattern formation given by the deterministic equations and induce complex spatiotemporal patterns that have not correctly been captured or predicted deterministically.

Traditionally pattern formation in chemical systems is mathematically described by deterministic nonlinear partial differential equations. This approach is to average out the spontaneous fluctuations in the microscopic degrees of freedom, giving a coarse-grained approximation of a more detailed microscopic or mesoscopic formulation. To take the internal fluctuations into consideration, one has to resort to a more fundamental description in which information pertaining to microscopic behavior is incorporated. For chemically reacting systems, such descriptions include mainly the approach of Langevin equation,[14,15] the chemical master equation formulation,[16] lattice-gas automata for reactive systems,[10] and the approach of microscopic simulation.[17]

At the level of mesoscopic description, pattern formation in chemical reaction−diffusion systems has been investigated using reactive lattice-gas models by Kapral and his colleagues.[10−12] A variety of media such as bistable, excitable, and oscillatory systems have been examined. Spatiotemporal structures such as wave propagations, spirals, Turing patterns, and fronts have been obtained. More recently, the influence of intrinsic fluctuations on pattern formation in mean-field reaction-diffusion models have been studied using Langevin-type equations.[13] Numerical simulations of the Langevin equations, which were constructed from the underlying master equation by mapping it to bosonic field theory,[18] demonstrated a drastically different picture from that predicted by the corresponding deterministic reaction-diffusion equations.

In this paper we choose the multivariate master equation of the Gray−Scott model to reexamine pattern formation. The formulation of the reaction−diffusion master equation is based on the local equilibrium assumption which is the central precondition for the extension of classic equilibrium thermodynamics to nonequilibrium thermodynamics.[16] The validity of the assumption and the reaction−diffusion master equation has been studied by Baras and Mansour.[19] Predictions obtained by the master equation were compared to that obtained by simulation of mesoscopic systems using Bird's algorithm. They found that multivariate master equation describes correctly realistic reaction−diffusion systems when the linear dimension of a cell is in the order of the reaction mean free path. We choose the reaction−diffusion master equation as our framework because it is elegant and simple, and is now numerically tractable with the advent of fast computers. The treatment of diffusion and computational issues involved in stochastic simulations of the multivariate master equation has also been addressed by different authors.[20,21] With the Gray−Scott model, we carry out

* Corresponding author. E-mail: qi@pku.edu.cn.
† Department of Physics, Peking University.
‡ The Beijing-Hong Kong-Singapore Joint Center for Nonlinear and Complex Systems (PKU).
§ Center for Theoretical Biology, Peking University.

10.1021/jp0674064 CCC: $37.00
Published on Web 01/26/2007

simulations of the underlying jump Markov processes of the master equation using Gillespie's algorithm, and examine mesoscopic pattern formation in comparison with deterministic results. The internal fluctuations are found to exhibit significant influence. They alter drastically the mean-field picture of pattern formation in the system. Complex spatiotemporal patterns, including spiral waves, Turing patterns, and self-replicating spots, which are not correctly predicted by the deterministic reaction−diffusion equations, are observed. Spatiotemporal behaviors such as patterns and wave propagations are controlled by the intensity of internal fluctuations. In the following, we first describe the model and methodology we adopt, then present the results obtained by direct simulation of the master equation in parallel with that of deterministic equations.

2. Model and Methodology

The Gray−Scott model[22] is a variant of the autocatalytic model of glycolysis proposed by Selkov.[23] It corresponds to the following reaction steps:

$$R_1:\ U + 2V \xrightarrow{k_1} 3V$$

$$R_2:\ V \xrightarrow{k_2} P$$

$$R_3:\ U \xrightarrow{k_3} Q$$

$$R_4:\ \xrightarrow{k_4} U \qquad (1)$$

The first reaction is an autocatalytic process in which a molecule of species U combined with two molecules of species V is converted catalytically to species V. The second and third reactions represent the decay of V and U into products P and Q, respectively. Species U is supplied constantly through the fourth reaction step. Both chemical species U and V diffuse with diffusion constants D_u and D_v. After rescaling, the kinetic reaction−diffusion equations for reactions (1) may be written as[24]

$$\frac{\partial u}{\partial t} = -uv^2 + F(1-u) + D_u\nabla^2 u$$

$$\frac{\partial v}{\partial t} = uv^2 - (F+k)v + D_v\nabla^2 v$$

where u and V represents the concentration of U and V, respectively. F and k are control parameters. Pattern formation in the deterministic reaction−diffusion eqs 2 and 3 has been investigated in detail in the past[24,28,30−32] and demonstrated very complex spatiotemporal patterns. Self-replicating spots have been described by Pearson.[24] The system was found to support Turing patterns,[28] localized structures or static spike autosolitons,[28,30] and spatiotemporal chaos.[30,31] The media can be excitable and generate spike spiral waves.[32]

The effect of noise in the Gray−Scott model attracted interest only recently. Gaussian white noise externally added to eqs 2 and 3 has been checked.[25] Solitary stable spots were found to be induced to elongate or self-replicate. Internal reaction noise has also been considered recently using approximate effective Langevin description.[13] Here we reexamine the pattern formation by directly simulating stochastically the microscopic master equation for the eqs 1.

The basic idea of the formulation is to divide the reaction volume into many spatial cells which are macroscopically small and microscopically large. Each cell is considered as well-mixed and is described by the numbers of reactive particles in it. The variables for each cell change as a result of two processes: chemical reactions, which are modeled by discrete Markov jumps, and diffusion, whereby a particle jumps to an adjacent cell as a Markov random walk. The time evolution of the stochastic system is then governed by the multivariate or reaction−diffusion master equation. This equation is overwhelmingly difficult for direct analysis. Therefore we resort to the approach of direct stochastic simulation.[26] This kind task of stochastic simulation of spatially distributed systems would probably be inconvenient in the past because it would cost a great deal of computer CPU time, but it is nowadays becoming practically applicable with the progress of fast computers.

For the Gray−Scott model, we assume that the species U and V react and diffuse stochastically on a two-dimensional lattice, which has been subdivided evenly into $N_x \times N_y$ square cells with size h. A cell on the lattice is indexed as (i,j), and the populations of the dynamical species in the cell are denoted as $U_{i,j}$ and $V_{i,j}$. The occurring reaction and diffusion transitions related with cell (i,j) can be listed as follows. (1) Reactions and propensities:

$$U_{i,j} + 2V_{i,j} \rightarrow 3V_{i,j},\quad \frac{k_1}{\Omega^2}U_{i,j}V_{i,j}(V_{i,j}-1)$$

$$V_{i,j} \rightarrow P \quad k_2 V_{i,j}$$

$$U_{i,j} \rightarrow Q \quad k_3 U_{i,j}$$

$$\rightarrow V_{i,j} \quad k_4 \Omega U_{i,j}$$

(2) Diffusive jump of U species with propensity $D_u U_{i,j}/h^2$:

$$U_{i,j} \rightarrow U_{i\pm1,j\pm1}$$

(3) Diffusive jump of V species with propensity $(D_v V_{i,j}/h^2)$:

$$V_{i,j} \rightarrow V_{i\pm1,j\pm1}$$

The constant Ω is introduced as a parameter for measuring and controlling the scale of population size. As internal noise is scaled with system size, molecule number fluctuations are significant in systems of finite number of molecules. A large (or small) value of Ω encompasses the system to have large (or small) number of particles, corresponding therefore to less (or more) intensive internal reaction noise in the system. By controlling the value of Ω, the strength of internal noise can be adjusted and the effect on pattern formation can be checked.

The above jump Markov processes of the whole system can be described by the reaction−diffusion master equation as given in ref 13. There are 12 transition channels (4 reaction steps, 8 diffusive jumps of species U and V) in each cell. The total number of reaction and diffusion channels on the lattice is $12 \times N_x \times N_y$ which is a large number for the lattice size. To achieve computational speedup when carrying out the simulation, we adopt the accelerated algorithm of Gillespie's direct method where the data structure for the channels of reaction and diffusion are organized into a binary tree. The approach known as K-level scheme[27] is very efficient in our simulations.

To compare stochastically simulated results with the counterpart of deterministic description, we take the parameters $k_1 = 1$, $k_2 = F + k$, $k_3 = F$, $k_4 = F$ for the reactions (1) according to eqs 2 and 3. Pattern formation predicted by eqs 2 and 3 are generated by numerical integration of the equations using the

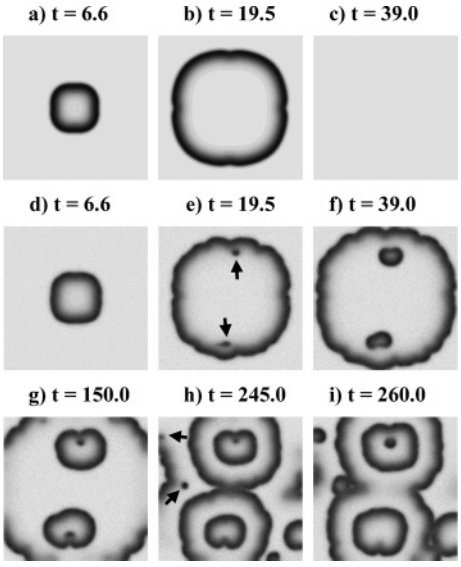

Figure 1. Wave nucleations activated by internal reaction noise. The time evolution of the wave initiated at the center predicted by the deterministic reaction−diffusion equations are shown in panels a−c; results generated from stochastic simulations are shown in panels d−i. Parameters are $k = 0.045$, $F = 0.015$, $D_u = 2.0 \times 10^{-5}$, $D_v = 10^{-5}$, $\Omega = 1500$, lattice $N_x = N_y = 200$ with spacing $h = 0.01$. The snapshots are generated by encoding U concentration by gray scales, with white and black corresponding to high and low concentration, respectively.

Heun algorithm.[3] For both stochastic simulation and numerical integration of the deterministic rate equations, zero-boundary conditions are applied. As the pattern formation generated depends on initial conditions, in the rest of this paper except for that pointed out explicitly, we adopt (following refs 24 and 25) the initial condition which consists of a localized square 10×10 pulse that perturbs the homogeneous steady state $U = 1$, $V = 0$.

3. Results

Neglecting the diffusion terms, eqs 2 and 3 give a trivial steady state (with $u = 1$, $v = 0$), referred to as red state, which is always stable. Another steady state, referred to as blue state (in the vicinity of $u = 0.3$, $v = 0.25$), is generated from a saddle-node bifurcation. The blue state can lose its stability through a Hopf or a Turing bifurcation. The bifurcation lines lie closely in the parameter plane.[28] It is in the neighborhood of these bifurcations that very complex spatiotemporal patterns have been reported.[24]

We reexamine the mesoscopic pattern formation by exploring systematically the $F - k$ parameter plane. Attention is payed to how internal reaction noises affect the dynamics and to the extent to which internal noise is capable of changing the patterns exhibited in the deterministic system. We observe that the intrinsic reaction fluctuations manifest prominent effect on the dynamical behavior of the system. They induce complex spatiotemporal patterns which are not captured or predicted correctly by eqs 2 and 3.

Figure 1 demonstrates the phenomenon of wave nucleation induced by internal noises. Under certain parameter values, the initial perturbation of the localized square pulse creates a wave in the central part of the media. The time evolution given by the deterministic reaction−diffusion equations shows that the wave spreads out and disappears after it propagates out of the boundaries, see Figure 1a−c. The system eventually recovers to the homogeneous red state (Figure 1c). In comparison, the corresponding stochastic simulation result, as shown in Figure 1d−i, depicts the behavior predicted by the master equation. One observes that before the initially activated wave front propagates out of the media, a pair of spiral waves are inspired. Arrows in the snapshots indicate the locations where new waves are activated. As the time proceeds, new waves are created continuously in a random manner. Because of the spontaneous nucleation of waves, the media is always oscillatory. Thus we find the phenomenon of internal-noise-induced chemical waves.

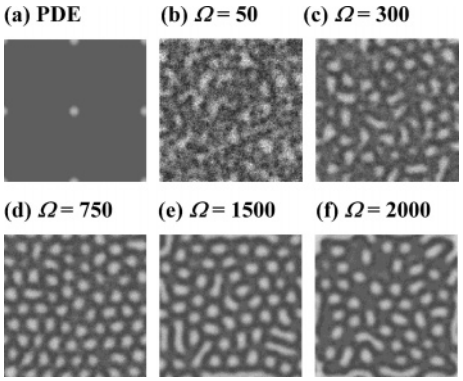

Figure 2. Deterministic localized structure (a) in comparison with stochastic simulations under different level of internal noise (b−f). With the value $\Omega = 750$, Turing pattern is induced (d). Parameters are $k = 0.06085$, $F = 0.06$. Lattice size $N_x = N_y = 128$. Other parameters are the same as with Figure 1.

The behavior we find here resembles the phenomenon of wave-induced chaos where spatiotemporal chaos arises from an initial traveling wave.[29] In our simulations, no active structures develop spontaneously before an initial wave passes through and disturb the system from its resting state. Therefore the behavior in Figure 1d−i is also wave-induced. The difference lies in that the creation of wave-induced chaos does not need the help of noise, whereas in our results the internal noise is essential. Numerical integration with reaction−diffusion eqs 2 and 3 without noise generates asymptotically the homogeneous red state despite whatever inhomogeneous initial conditions are used.

The random activation of waves by the intrinsic noise is related with Ω. As Ω decreases, the populations of species U and V decrease and therefore stronger internal fluctuations are presented in the system. In this circumstance, the simulation with a decreased Ω shows that molecular noise can activate waves more frequently. When Ω is sufficiently small, wave propagation is ruined by the dense and random activations; the media turns into an irregularly fluctuating pattern. On the other hand, as Ω increases the fluctuation weakens. When Ω is at 4000, the internal noise is still able to activate wave propagations. In the limit as Ω grows to infinity, the simulated behavior is expected to approach the deterministic result.

Internal molecular fluctuations can drastically change localized structures given by the deterministic equations. Figure 2a shows the localized pattern obtained by direct integration of eqs 2 and 3 with the initial condition of central-pulse perturbation in the bistable regime. The asymptotic pattern is temporally static with the localized red-state spots surrounded by the blue-state environment. The effect of internal noise depends on the noise strength. When the simulation is performed with $\Omega = 50$, which corresponds to a relatively strong noise, the localized steady structure collapses, and irregular fluctuating patterns or *thermal patterns* are generated (Figure 2b). The patterns are called *thermal* because they are irregular and are sustained by the internal fluctuations. As Ω grows (Figure 2c), red-state spots are activated. But the spots are not static; they fluctuate around

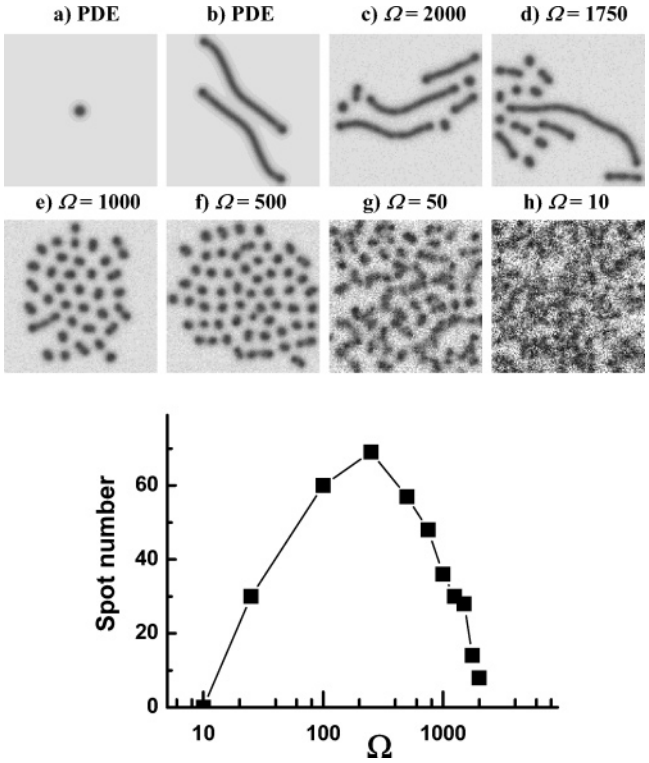

Figure 3. Internal noise induced self-replicating spots. Panels a and b show results of the partial differential eqs 2 and 3. Stochastically simulated results with different Ω are presented in panels c−h. The bottom curve shows the dependence of spot numbers on Ω. Parameters are $k = 0.065$, $F = 0.05$, lattice $N_x = N_y = 128$, $h = 0.01$; simulation time $t = 10000$.

where they are born and are annihilated after some time under the influence of molecular fluctuations. Simulated patterns with a larger value of Ω are more regular. At an optimum value around Ω = 750, the pattern becomes regular hexagons. It is stationary both in space and time (Figure 2d. We thus obtain a Turing pattern induced by internal noises. Simulations with even larger Ω show that the patterns are still temporally stable, but are distorted from the hexagonal pattern (Figure 2e). As Ω is increased further, the spots in the simulated pattern become sparser (Figure 2f). The pattern would finally approach the deterministic localized pattern as Ω becomes large enough.

The initial condition of localized stimulus that we apply to eqs 2 and 3 can evolve into a temporally static and radially symmetric solitary spot under proper parameters,[30] as shown in Figure 3a. If the initial condition is randomly disturbed slightly, elongated strips that grow in preferred directions are generated (Figure 3b). The deterministic picture is changed drastically in the stochastic simulations. When the simulation is performed with a large Ω (weak internal noise), the resulting elongated strips still grow (see Figure 3c). But occasionally the growth is interrupted by fluctuations, and spots are severed from the growing tips. The spots can also evolve into strips which can also be broken. As the internal noise level grows, the strips rupture into short pieces or spots (Figure 3d). Simulations with a sufficient small value of Ω generate the pattern of self-replicating spots (Figure 3e,f), which have been well-known in the deterministic Gray−Scott model.[24] The spot-replicating rate increases with the increase of the fluctuation strength. As Ω becomes small enough, the spot pattern will be ruined. It will be completely smeared out when the fluctuations are too intensive. The bottom plot in Figure 3 depicts the number of spots and strips for the evolution time $t = 10000$ as a function

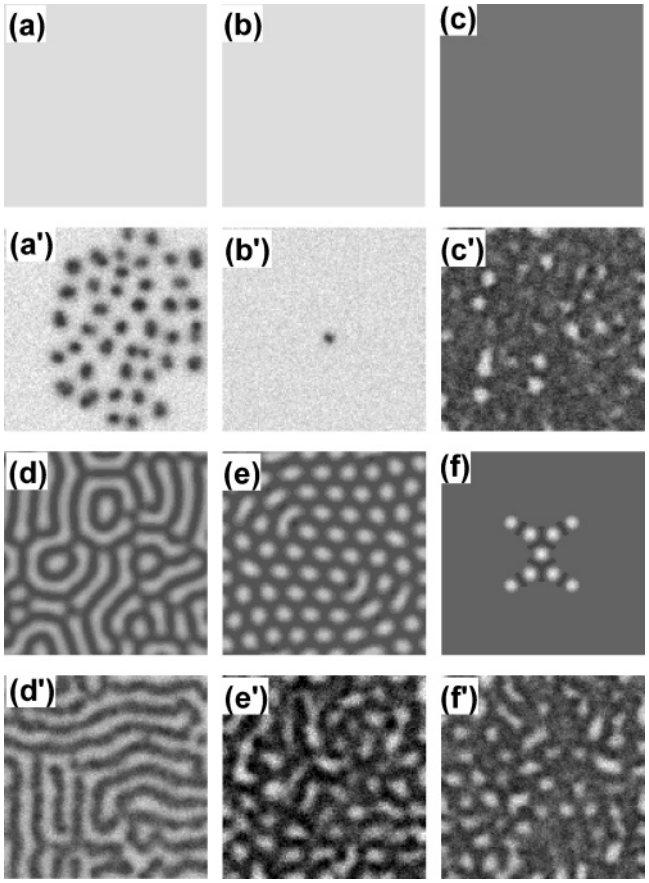

Figure 4. Spatiotemporal patterns predicted by eqs 2 and 3 (a−f) in comparison with the results of direct stochastic simulation of the multivariate master equation (a′−f′). Parameters are $k = 0.065$, $F = 0.035$ for (a, a′); $k = 0.0675$, $F = 0.06$ for (b, b′); $k = 0.06$, $F = 0.07$ for (c, c′); $k = 0.06$, $F = 0.04$ for (d, d′); $k = 0.055$, $F = 0.03$ for (e, e′); $k = 0.06$, $F = 0.05$ for (f, f′); Ω = 300, lattice size $N_x = N_y = 128$. Other parameters are the same as with Figure 1.

of Ω. The bell-shaped curve demonstrates an optimal level of internal noise, which bears similarities to the phenomenon of stochastic resonance. The phenomenon of spot replication controlled by intrinsic fluctuations is analogous to the results demonstrated in ref 25 with Langevin equations, where the Gaussian white noise that controlled the same pattern dynamics was externally introduced to the deterministic equations.

As we explore the $F - k$ parameter space, we observe that the manifestation of intrinsic fluctuations on pattern formation is extensive. Besides those described above, internal noise-induced drastic changes of the patterns exhibited by the deterministic system are summarized in Figure 4. The patterns in Figure 4a−f are produced by numerical integration of eqs 2 and 3, while the panels a′−f′ are generated by stochastic simulations with same parameters to panels a, b, c, d, e, and f, respectively. One sees that the asymptotic behaviors predicted by eqs 2 and 3 can be homogeneous red state (Figure 4a,b) or blue state (Figure 4c). The stochastic simulations demonstrate, however, self-replicating spots (Figure 4a′), solitary stable spot (Figure 4b′), and fluctuating thermal patterns of spot spontaneously generated (Figure 4c′), respectively. Deterministic results such as spot-strip mixtures (Figure 4d), Turing patterns (Figure 4e), and localized structures (Figure 4f) turns into lacelike patterns (Figure 4d′), fluctuating spot patterns (Figure 4e′,f′) in stochastic simulations, respectively.

Figure 5 illustrates the stochastically simulated phase diagram in the $F - k$ parameter plane. The patterns designated by Greek

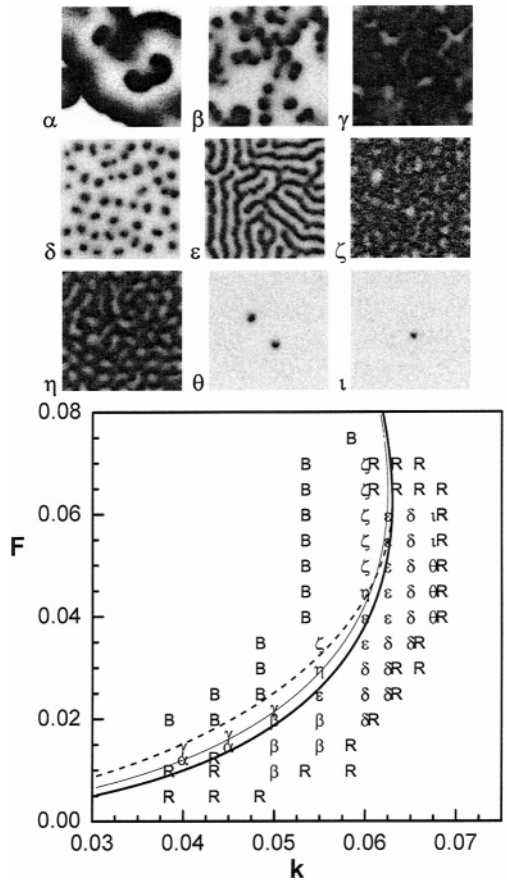

Figure 5. Stochastically simulated patterns indicated by Greek letters and their locations in the $F-k$ parameter space. The bold solid line is the saddle-node bifurcation curve. The dashed line and the thin solid curve indicate the Hopf instability and the Truing bifurcation of the blue state, respectively. The map has been calculated by simulations with parameters $\Omega = 300$, $D_u = 2 \times 10^{-5}$, $D_u = 2 \times 10^{-5}$. $N_x = N_y = 128$.

letters are produced from simulations with $\Omega = 300$ for $t = 15000$. Greek characters in the parameter plane indicate the pattern found at that point. Pattern α is the fluctuation-activated wave pattern similar to those in Figure 1. Patterns β and γ are spatiotemporal chaos. The simulated self-replicating spot is designated with δ which is also chaotic. The lacelike or labyrinthine pattern ϵ evolves very slowly with time. Letter ζ indicates an irregular spontaneously fluctuating thermal pattern, and η denotes spot patterns that are driven by the underlying fluctuations. A solitary stable spot can also be simulated as indicated by θ and ι. All these results are computed for a single set of initial conditions, namely, the homogeneous red state perturbed with the localized square. For a given parameter set there will be multiple possible solutions and different patterns can be obtained if the initial conditions are varied. The pattern map in the parameter space would therefore be different as the simulations are performed with other kinds of initial conditions. In comparison with the deterministic map reported in ref 24, complex spatiotemporal patterns given by the mesoscopic description still come out in the neighborhood of the bifurcation lines, but the phase diagrams are drastically changed by internal reaction noises. Several types of pattern such as stripes, self-replicating spots, and spatiotemporal chaos are preserved in the master equation description, but the regimes in the parameter space is changed.

The above results are obtained from simulations with the ratio $D_u/D_v = 2$ of the two diffusion constants. As reported in ref 32, the deterministic Gray−Scott model can also be excitable, and rotating spiral waves, called spike spiral waves, can be produced. We performed stochastic simulations of spiral waves in this excitable regime. The results are presented in Figure 6. Figure 6b is the deterministic spiral wave evolved from the initial condition of Figure 6a. Figure 6 parts c−f are produced from stochastic simulations with different values of Ω. When Ω is very small (Figure 6c,d), the local populations of species U and V in the cells are very small, typically with one to four particles of U species and even a less number of V species. The fluctuation is therefore very intensive. Because of the fluctuations, the spiral wave fails to nucleate; the initially prepared narrow wave front is quickly destroyed by the intensive fluctuations, and randomly activated *thermal-wave* patterns, which are fuzzy and have fairly irregular shapes, are produced spontaneously (Figure 6c). The word *thermal wave* has been coined originally to describe irregularly activated waves in subexcitable media by external noises.[33] The thermal wave fronts we observe here are, however, sustained inherently in the system by the intrinsic noises. With $\Omega = 4$, a target wave can form by chance (Figure 6d). In this case, the system locks to the homogeneous red state after the wave propagates out of the media. As Ω grows and fluctuations decrease, the waves are able to nucleate but occasionally interrupted by the fluctuations (Figure 6e). A full spiral is produced with $\Omega = 15$ (Figure 6f), locally with at most fifteen U particles and about nine V particles. Considering that the particle numbers of both species for each cell are still very low and the fluctuations are intensive, the spiral wave is quite robust to internal fluctuations. This is in accordance with the results of lattice-gas automata reported by Kapral et al.[10−12] The result obtained from the stochastic simulation with $\Omega = 500$ turns out to be in very good agreement with the deterministic spiral. In the stochastic simulation, we notice that the wave propagation is hindered by the intrinsic fluctuations: the waves in the stochastic media propagate with a slower speed in comparison with the deterministic behavior. The higher is the level of internal fluctuations, the slower is the wave speed.

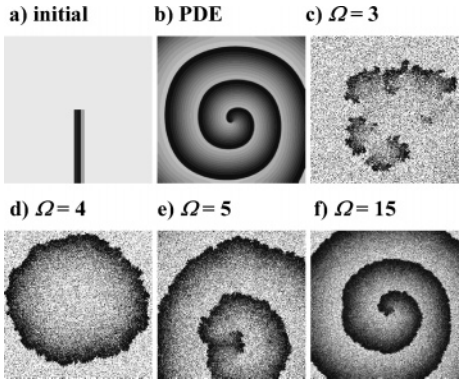

Figure 6. Effect of internal noise on the nucleation of a spiral wave in the excitable regime. Snapshots in panels c−f with $\Omega = 3$, 4, 5, 15, respectively, are generated from stochastic simulations. Panel a shows the initial condition for both stochastic and deterministic calculations. The deterministic spiral (b) is produced by numerical integration of the partial differential eqs 2 and 3. Parameters are $k = 0.0225$, $F = 0.0025$, $D_u = 0$, $D_v = 0.005$, $t = 3000$, lattice $N_x = N_y = 256$ with spacing $h = 0.3$.

Another influence of internal noise we notice in our stochastic simulations is that the inherent noise can change the dominance of the two bistable states. In the bistable regime of the model, one can initially prepare half of the media in the red state and the other half in the blue state. The front between the two regions can invade the two states. Simulations (results not shown here)

with different values of Ω show that the invading direction and speed of the front is controlled by the intensity of the underlying fluctuations.

4 Discussion

We have reported stochastic simulations of mesoscopic pattern formation in the Gray−Scott model in the framework of reaction−diffusion master equation. The deterministic pattern formation has been found to be drastically changed owing to the influence of internal reaction noise which is inherent to the system. Fruitful patterns which are not captured or correctly predicted by the deterministic kinetics have been induced by intrinsic fluctuations. Such patterns have included the waves or spirals, self-replicating patterns, Turing patterns, solitary stable spots, and thermal patterns of waves or spots et al. Furthermore, the pattern formation is controlled by the fluctuation strength. Encompassed by controlling the value of Ω, the system manages to select different patterns. The results presented here indicate that intrinsic noise inherent to genuine systems can select and control complex pattern formations of potential biological and chemical significance.

The results we reported here from direct stochastic simulation of the master equation are quite different from that reported in a recent parallel work, which has considered the Langevin equation approximation of the multivariate master equation.[13] In our simulations some of the deterministic patterns such as self-replicating spots, strips, and spatiotemporal chaos survive the intrinsic fluctuations. Their numerical results from the Langevin equation description showed that none of the noise-free patterns reported in ref 24 survived in the Langevin equation description. Instead, some irregular time-dependent patterns were produced. The pattern map in the parameter space reported in ref 13 bears little similarity to the map (Figure 5) we report here. In our simulations, the map depends on the strength of internal fluctuations, and the simulation results approach the deterministic map as Ω becomes large enough.

As the noise level is scaled with the system size, the stochastic effect is significant and important in systems with a finite number of molecules such as in biological intracellular processes. In living cells, when there are species such as DNA and important regulatory molecules having very few copy numbers, the effects of noise may account for cell to cell variation and play important roles in biological processes.[34] On the other hand, thermal waves activated by external Gaussian white noise has been used to account for brain calcium waves observed in cultured networks of hippocampal rat-brain astrocytes.[35] The fact we find here that thermal waves can be activated in excitable media inherently by the intrinsic fluctuations suggests that the brain calcium waves might also possibly be explained by the influence of internal noise without the help of a fluctuating environment. Similarly, the intrinsic fluctuations due to a finite number of molecules in living cells might have played a role in intracellular pattern formation such as intracellular calcium waves[36] and calcium patterns.[37] The calcium waves might be activated, or at least influenced, by internal reaction fluctuations as our stochastic simulation with the Gray−Scott model has indicated (see Figure 1). Calcium is a vital and universal second messenger which plays versatile roles in many inter- and intracellular processes;[38] investigations of the effect of intrinsic fluctuations on the formation of calcium oscillations and wave patterns are desirable in future studies.

Acknowledgment. This work is partially supported by the Chinese Natural Science Foundation and Department of Science of Technology in China.

References and Notes

(1) Horsthemke, W.; Lefever, R. *Noise-Induced Transitions*; Springer: Berlin, 1984.

(2) Gammaitoni, L.; Hanggi, P.; Jung, P.; Marchesoni, F. *Rev. Mod. Phys.* **1998**, *70*, 223.

(3) García-Ojalvo, J.; Sancho, J. M. *Noise in Spatially Extended Systems*; Springer: New York, 1999.

(4) Van, den Broeck, C.; Parrondo, J. M.; Toral, R. *Phys. Rev. Lett.* **1994**, *73*, 3395.

(5) (a) Bucetal, J.; Ibañes, M.; Sancho, J. M.; Lindenberg, K. *Phys. Rev. E* **2003**, *67*, 021113. (b) Wood, K.; Buceta, J.; Lindenberg, K. *Phys. Rev. E* **2006**, *73*, 022101. (c) Wang, H.; Zhang, K.; Ouyang, Q. *Phys. Rev. E* **2006**, *74*, 036210 .

(6) (a) Santos, M. A.; Sancho, J. M. *Phys. Rev. E* **1999**, *59*, 98. (b) Zhou, L. Q.; Jia, X.; Ouyang, Q. *Phys. Rev. Lett.* **2002**, *88*, 138301.

(7) (a) Jung, P.; Mayer-Kress, G. *Phys. Rev. Lett.* **1995**, *74*, 2130. (b) Alonso, S.; Sendiña-Nadal, I.; Pérez-Muñuzuri, V.; Sancho, J. M.; Sagués, F. *Phys. Rev. Lett.* **2001**, *87*, 078302.

(8) (a) Wang, H.; Ouyang, Q. *Phys. Rev. E* **2002**, *65*, 046206. (b) Wang, H. *Phys. Rev. Lett.* **2004**, *93*, 154101. (c) Wang, H.; Ouyang, Q. *Chaos* **2005**, *15*, 023702.

(9) See for instance: (a) Geysermans, P.; Baras, F. *J. Chem. Phys.* **1996**, *105*, 1402. (b) Wang, H. *J. Chem. Phys.* **2001**, *114*, 5099. (c) Shuai, J. W.; Jung, P. *Phys. Rev. Lett.* **2002**, *88*, 068102. (d) Gong, Y. B.; Hou, Z.; Xin, H. *J. Phys. Chem. B* **2004**, *108*, 17796. (e) Escudero, C.; Buceta, J.; de la Rubia, F. J.; Lindenberg, K. *Phys. Rev. E* **2004**, *70*, 061907.

(10) Boon, J. P.; Dab, D.; Kapral, R.; Lawniczak, A. *Phys. Rep.* **1996**, *273*, 55.

(11) Voroney, J.; Lawniczak, A.; Kapral, R. *Physica D (Amsterdam)* **1996**, *99*, 303.

(12) Kapral, R.; Wu, X. G. *J. Phys. Chem.* **1996**, *100*, 18976.

(13) Hochberg, D.; Zorzano, M. P.; Moran, F. *J. Chem. Phys.* **2005**, *122*, 214701.

(14) Nitzan, A.; Ortoleva, P.; Deutch, R.; Ross, J. *J. Chem. Phys.* **1974**, *61*, 1056.

(15) Hochberg, D.; Zorzano, M.-P.; Moran, F. *Phys. Rev. E* **2006**, *73*, 066109.

(16) Nicolis, G.; Prigogine, I. *Self-Organization in Nonequilibrium Systems*; Wiley-Interscience: New York, 1977.

(17) Bird, G. A. *Molecular Gas Dynamics*; Clarendon: Oxford, 1976.

(18) Doi, M. *J. Phys. A: Math. Gen.* **1976**, *9*, 1465.

(19) Baras, F.; Mansour, M. M. *Phys. Rev. E: Stat. Phys., Plasmas, Fluids, Relat. Interdiscip. Top.* **1996**, *54*, 6139.

(20) Stundzia, A. B.; Lumsden, C. J. *J. Comput. Phys.* **1996**, *127*, 196.

(21) Bernstein, D. *Phys. Rev. E: Stat. Phys., Plasmas, Fluids, Relat. Interdiscip. Top.* **2005**, *71*, 041103.

(22) Gray, P.; Scott, S. K. *Chem. Eng. Sci.* **1984**, *39*, 1087.

(23) Selkov, E. E. *Eur. J. Biochem.* **1968**, *4*, 79.

(24) Pearson, J. E. *Science* **1993**, *261*, 189.

(25) Lesmes, F.; Hochberg, D.; Moran, F.; Perez-Mercader, J. *Phys. Rev. Lett.* **2003**, *91*, 238301.

(26) (a) Gillespie, D. T. *J. Phys. Chem.* **1977**, *81*, 2340. (b) Gillespie, D. T. *J. Chem. Phys.* **2001**, *115*, 1716.

(27) Blue, J. L.; Beichl, I. *Phys. Rev. E: Stat. Phys., Plasmas, Fluids, Relat. Interdiscip. Top.* **1995**, *51*, R867.

(28) Mazin, W.; Rasmussen, K. E.; Mosekilde, E.; Borckmans, P.; Dewel, G. *Math. Comput. Simulat.* **1996**, *40*, 371.

(29) Merkin, J. H.; Petrov, V.; Scott, S. K.; Showalter K. *Phys. Rev. Lett.* **1996**, 76, *546*.

(30) Muratov, C. B.; Osipov, V. V. *Eur. Phys. J. B* **2001**, *22*, 213.

(31) Nishiura, Y.; Ueyama, D. *Physica D (Amsterdam)* **2001**, *150*, 137.

(32) Muratov, C. B.; Osipov, V. V. *Phys. Rev. E: Stat. Phys., Plasmas, Fluids, Relat. Interdiscip. Top.* **1999**, *60*, 242.

(33) Jung, P. *Phys. Rev. Lett.* **1997**, *78*, 1723.

(34) (a) Arkin, A.; Ross, J.; McAdams, H. *Genetics* **1998**, *149*, 1633. (b) Elowitz, M.; Levine, A.; Siggia, E.; Swain, P. *Science* **2002**, *297*, 1183. (c) Qian, H. *J. Phys. Chem. B* **2006**, *110*, 15063.

(35) Jung, P.; Cornell-Bell, A.; Madden, K. S.; Moss, F. *J. Neurophysiol.* **1998**, *79*, 1098.

(36) Dawson, S. P.; Keizer, J.; Pearson, J. E. *Proc. Natl. Acad. Sci. U.S.A.* **1999**, *96*, 6060.

(37) Créton, R.; Speksnijder, J. E.; Jaffe, L. F. *J. Cell Sci.* **1998**, *111*, 1613.

(38) Berridge, M. J.; Lipp, P.; Bootman, M. D. *Nat. Rev. Cell. Biol.* **2000**, *1*, 11.